

## Vibrating-wire measurement method for centering and alignment of solenoids

This content has been downloaded from IOPscience. Please scroll down to see the full text.

2013 JINST 8 P11006

(<http://iopscience.iop.org/1748-0221/8/11/P11006>)

View [the table of contents for this issue](#), or go to the [journal homepage](#) for more

Download details:

IP Address: 84.97.66.88

This content was downloaded on 02/02/2015 at 08:50

Please note that [terms and conditions apply](#).

## Vibrating-wire measurement method for centering and alignment of solenoids

P. Arpaia,<sup>a,b,1</sup> C. Petrone,<sup>a,b</sup> S. Russenschuck<sup>b</sup> and L. Walckiers<sup>b</sup>

<sup>a</sup>Department of Engineering, University of Sannio,  
Corso Garibaldi 107, 82100 Benevento, Italy

<sup>b</sup>CERN, Department of Technology, Group of Magnets, Superconductors and Cryostats (MSC),  
Section of Magnetic Measurements, 1211 Geneva 23, Switzerland

E-mail: [arpaia@unisannio.it](mailto:arpaia@unisannio.it)

**ABSTRACT:** A method is proposed to center and align solenoids by means of a vibrating wire. The magnetic axis of a solenoid is defined as the path where the integral over the transversal field components takes its minimum. The wire, fed by an alternating current, oscillates in a plane that is perpendicular to the transversal magnetic field. When the wire position coincides with the magnetic axis, the transversal field components cancel out and therefore no motion is induced. To center and align the solenoid two wire resonance frequencies are excited for co- and counter-directional movements of the wire stages. The procedure to find the minimum oscillation amplitudes is sensitive to misalignment in the micrometer range. The experimental validation was carried out on a solenoid for the linear accelerator Linac4 at CERN.

**KEYWORDS:** Instrumentation for particle accelerators and storage rings - high energy (linear accelerators, synchrotrons); Hardware and accelerator control systems; Accelerator Subsystems and Technologies; Beam-line instrumentation (beam position and profile monitors; beam-intensity monitors; bunch length monitors)

<sup>1</sup>Corresponding author.

---

## Contents

<b>1</b>	<b>Introduction</b>	<b>1</b>
<b>2</b>	<b>Measurement of the magnetic-axis position</b>	<b>2</b>
2.1	The analytical description of the method	2
2.2	The measurement principle	4
2.2.1	Co-directional search	4
2.2.2	Counter-directional search	6
2.3	The measurement procedure	6
<b>3</b>	<b>Experimental validation of the method</b>	<b>8</b>
3.1	The measurement system	8
3.2	Experimental results	11
<b>4</b>	<b>Conclusions</b>	<b>13</b>

---

## 1 Introduction

Short solenoidal lenses are used as focusing elements in electron microscopes and other electron beam devices. In particle accelerators, the beam-emittance growth is reduced by axially-symmetric magnetic elements arranged in lattices of short periods. This arrangement often works better than sequential pairs of quadrupoles, which give rise to significant halo formation [1]. Particles moving exactly along the magnetic axis of the solenoids are not deflected. Conversely, off-axis particles are azimuthally accelerated by the radial field component in the end regions of the magnet. The resulting helical motion in the longitudinal field region of the magnet yields a focusing effect due to the radial Lorentz force.

A key performance issue in solenoid testing is the accurate determination of the magnetic axis. This is also a prerequisite for measuring the symmetry of the magnetic field and possible manufacturing errors. The magnetic axis of a solenoid is defined as the path where the integral over the transversal field components takes its minimum. A classical method is to map the field by a Hall probe, mounted on a three-axis coordinate stage controlled by a computer; a relatively slow process that relies on sturdy mechanics of the stage and a good calibration and thermalization of the probe.

The magnetic axis position can be measured also by means of the classical single stretched-wire method [2]. An electrical voltage is induced across a wire displaced in a magnetic field. The difference in the integrated voltages for two wire displacements in opposite directions yields the offset of the starting point with respect to the magnetic axis. Although this method works well for quadrupole magnets [3], the sensitivity is much lower for solenoid magnets because the intercepted transversal field components are present only in the fringe field regions of the magnet.

Powering the wire by an alternating current yields a relatively large oscillation amplitude, if the field integral along the wire, and thus the total Lorentz force on the wire, does not vanish. Due to this increased sensitivity, the vibrating wire method is usually exploited to measure magnetic axes position and longitudinal field profiles in quadrupole accelerator magnets [4]. The measurement sensitivity is maximized by setting the alternating current frequency to the natural resonance frequency of the wire [5]. The magnetic axis is determined by finding the wire position in the magnet aperture where the oscillations at first and second resonance frequencies takes their minimum. A quadrupole can be centered at the micrometer level and the pitch and yaw angles can be measured to the milli-radian level.

In this paper, a method based on the vibrating-wire method is proposed for measuring the position of the magnetic axis of a solenoid. In particular, section 2 contains the analytical description of the method, the measurement principle, and the measurement procedure. Section 3 covers the validation of the measurement method and gives experimental results obtained for a solenoid magnet for the linear accelerator Linac4 at CERN.

## 2 Measurement of the magnetic-axis position

### 2.1 The analytical description of the method

The magnet centering and alignment principle is based on intercepting the transverse field components [6, 7]. To this end, consider the coordinate system as shown in figure 1. A stretched wire with fixed points at  $z = 0$  and  $z = L$  is supplied by an alternating current  $I(t) = I_0 \sin(\omega t)$  and therefore oscillates in a plane perpendicular to the transverse components of the magnetic flux density  $\mathbf{B}$ . The wire oscillation is proportional to the wire current amplitude  $I_0$  and to the field strength. The steady-state solution of the wire motion is given by

$$y(z, t) = \frac{2I_0}{L} \sum_m \frac{\int_0^L B_x(z) \sin\left(\frac{m\pi}{L}z\right) dz}{\sqrt{\left[T\left(\frac{m\pi}{L}\right)^2 - \rho\omega^2\right]^2 + (\alpha\omega)^2}} \sin\left(\frac{m\pi}{L}z\right) \sin(\omega t - \varphi_m), \quad (2.1)$$

where  $\rho$  is the mass per unit length,  $[\rho] = 1 \text{ kg m}^{-1}$ ,  $\alpha$  the damping coefficient,  $[\alpha] = 1 \text{ kg m}^{-1} \text{ s}^{-1}$ , and  $T$  is the tension in the wire,  $[T] = 1 \text{ N} = 1 \text{ kg m s}^{-2}$ . By defining the modal force

$$F_m := \int_0^L I_0 B_x(z) \sin\left(\frac{m\pi}{L}z\right) dz, \quad (2.2)$$

the mode-shape function

$$Y_m(z) := \sin\left(\frac{m\pi}{L}z\right), \quad (2.3)$$

and the nodal displacement

$$q_m(t) := \sin(\omega t - \varphi_m), \quad (2.4)$$

and using the resonance frequency condition  $\omega_m = 2\pi f_m = \frac{m\pi}{L} \sqrt{\frac{T}{\rho}}$ , eq. (2.1) can be written as

$$y(z, t) = \frac{2}{L} \sum_m \frac{F_m Y_m(z) q_m(t)}{\sqrt{[\rho(\omega_m^2 - \omega^2)]^2 + (\alpha\omega)^2}}. \quad (2.5)$$

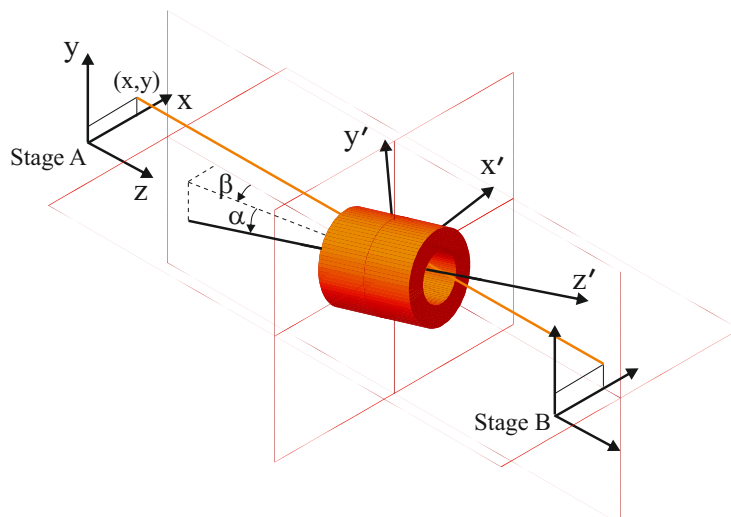


**Figure 1.** Coordinate systems of the magnet with pitch (tilt)  $\alpha$  and yaw (swing)  $\beta$  angles [9].

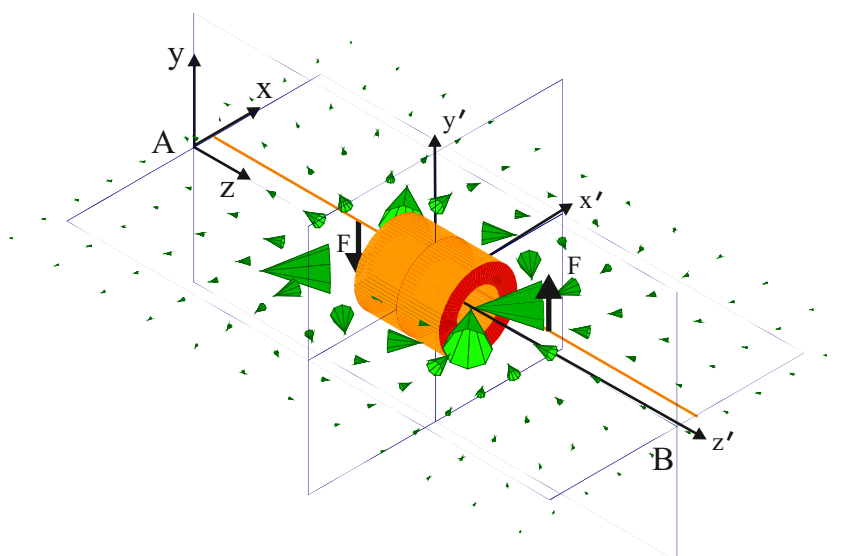


**Figure 2.** Stray field on the horizontal plane and direction of the Lorentz force, simulated with the CERN field computation program ROXIE [9].

Without loss of generality, the wire is considered to be misaligned with respect to the magnetic axis only in the horizontal plane. The fringe fields in this plane, shown for a numerical simulation in figure 2, give rise to a Lorentz force in the vertical direction  $y$ . When the magnetic axis coincides with the wire position, the integral of the transverse magnetic field components along the wire vanishes and thus the wire oscillation takes its minimum.

## 2.2 The measurement principle

The position of the magnetic axis is defined by the four transversal coordinates at the wire stages, which are labelled as  $A$  at  $z = 0$  and  $B$  at  $z = L$ . The transversal coordinates are assembled in the design variable vector  $\mathbf{X} := (x_A, y_A, x_B, y_B)$ . The position of the magnetic axis is obtained by minimizing an objective function  $f : \mathbb{R}^4 \rightarrow \mathbb{R} : \mathbf{X} \mapsto f(\mathbf{x})$ , where  $f$  is the RMS value of the two wire displacements in the horizontal and vertical planes,  $d_x(z_0)$  and  $d_y(z_0)$ , at a fixed position  $z_0$ . The search for the solenoid magnetic axis, expressed as a minimization problem, can then be written as  $\min_{\mathbf{X}} f(\mathbf{X})$ . This minimization problem is solved by successive one-dimensional searches, usually referred to as line searches.

The wire displacements  $d_x$  and  $d_y$  are proportional to the Lorentz force on the wire and depend upon the position  $\mathbf{X} := (x_A, y_A, x_B, y_B)$ , as shown schematically in figure 2. The displacements at a given longitudinal position  $z_0$ , are determined by measuring the peak-to-peak wire oscillation amplitudes in orthogonal directions,  $\delta_x$  and  $\delta_y$ , together with the phase differences  $\gamma_x$  and  $\gamma_y$  between the voltages from the displacement sensors and the voltage across a reference resistance conducting the excitation current:

$$d_x = \delta_x \operatorname{sign}\left(\gamma_x - \frac{\pi}{2}\right), \quad d_y = \delta_y \operatorname{sign}\left(\gamma_y - \frac{\pi}{2}\right). \quad (2.6)$$

The search quality and the measurement sensitivity are increased by alternating between two different search directions and wire resonance frequencies: (i) motion parallel in both  $x$  and  $y$  directions, that is, by a *co-directional* wire movement [8] where the wire is excited at its second resonance frequency, (ii) motion anti-parallel in both  $x$  and  $y$  directions, that is, by a *counter-directional* movement where the wire is excited at its fundamental resonance frequency. The first step, subsequently referred to as *centering*, yields a local minimum, while the second step, referred to as *alignment*, yields the global minimum. The steps must be iterated because the magnet center may also be displaced in longitudinal direction with respect to the wire center at  $z = L/2$ .

The measurement uncertainty increases for wire positions close to the magnetic axis, owing to the vanishing wire oscillation. A linear regression allows therefore the minimum in each line search to be found with a higher accuracy. The linear regression is furthermore motivated by the fact that the Cartesian field components in solenoid magnets vary linearly with the radial distance from the magnetic axis. Both the co- and counter-directional line searches are based on a linear regression of the measured signal.

### 2.2.1 Co-directional search

In a co-directional movement, both the wire extremities at  $z = 0$  and  $z = L$  are moved by the same displacement vector  $(x, y)$ , that is,  $\mathbf{X}_n = \mathbf{X}_{n-1} + (x, x, y, y)$ . By exciting the wire with a current at the second resonance frequency, the Lorentz forces are in phase with the wire oscillation on both the sides of the magnetic center. In this case, the wire motion is described as

$$y(z, t) = \frac{2I_0}{L\alpha\omega} Y_2(z) q_2(t) \int_0^L B_x(z) \sin\left(\frac{2\pi}{L}z\right) dz, \quad (2.7)$$

where  $Y_2(z)$  and  $q_2(t)$  are defined in eqs. (2.3) and (2.4), respectively.

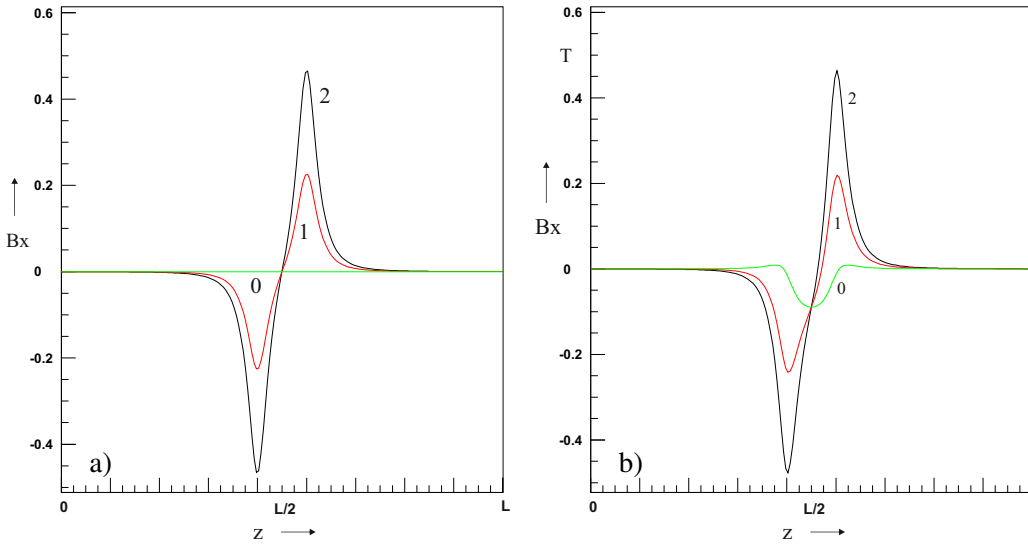


**Figure 3.** Simulated distribution of the transverse field component along the stretched wire from  $z = 0$  to  $z = L$ : a) Without pitch and yaw. b) With yaw angle of  $1.0^\circ$ .

**Table 1.** Values of the coefficients  $\mathcal{U}_k$  at the second resonance frequency.

$\mathcal{U}_1$	$1.0890 \times 10^{-8}$	$\mathcal{U}_2$	$6.1789 \times 10^{-5}$
$\mathcal{U}_3$	$4.3313 \times 10^{-9}$	$\mathcal{U}_4$	$2.8040 \times 10^{-8}$
$\mathcal{U}_5$	$4.4844 \times 10^{-10}$	$\mathcal{U}_6$	$1.2290 \times 10^{-8}$
$\mathcal{U}_7$	$3.1706 \times 10^{-11}$	$\mathcal{U}_8$	$6.3699 \times 10^{-9}$
$\mathcal{U}_9$	$1.1652 \times 10^{-10}$	$\mathcal{U}_{10}$	$3.3773 \times 10^{-9}$

The wire is centered with respect to the magnetic axis when the two fringe field effects cancel out and the oscillation amplitude takes its minimum. Figure 3 shows the simulated field profiles along the wire routed through the solenoid magnet from the stage A to stage B. Figure 3 (a) shows the situation for a perfect alignment of the magnet, i.e., both the pitch and yaw angles are zero. Notice the change in field direction on the left and right of the magnetic center. Figure 3 (b) shows the situation when a yaw misalignment is present (yaw angle  $\beta = 1.0^\circ$ ). Even if the wire is centered and the oscillation takes its minimum, a transversal fringe-field component remains in the same direction, left and right of the magnetic center.

Table 1 lists the amplitude coefficients

$$\mathcal{U}_m := \frac{2}{L} \frac{F_m}{\sqrt{[\rho(\omega_m^2 - \omega^2)]^2 + (\alpha\omega)^2}} \quad (2.8)$$

at the second resonance frequency, calculated for the field distribution according to figure 3 (a). The higher-order harmonics (overtone) are at least three orders of magnitude smaller, which justifies the use of the second wire resonance and the assumptions made in eq. (2.7).

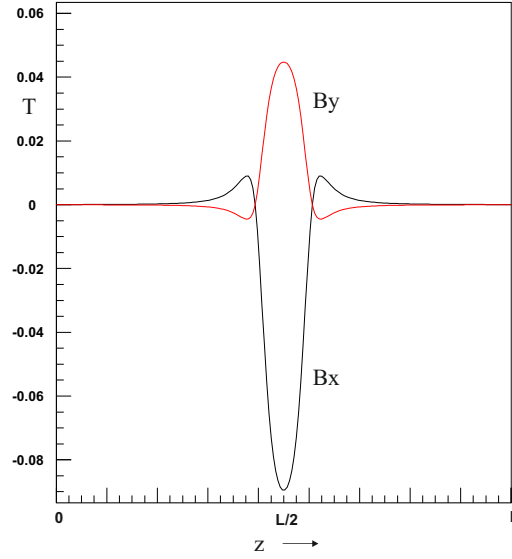


**Figure 4.** Simulated distribution of the transverse field component along the stretched wire for a perfectly centered, but misaligned solenoid ( $1.0^\circ$  yaw and  $0.5^\circ$  pitch).

### 2.2.2 Counter-directional search

Even when the local minimum is found by co-directional movement, residual pitch ( $\alpha$ ) and yaw ( $\beta$ ) angle misalignments may still exist. In this case, the fringe-field components point into the same direction left and right of the magnet center. The wire is therefore excited at its first resonance so that the wire motion in the vertical plane is proportional to  $\int_0^L B_x(z) \sin\left(\frac{\pi}{L}z\right) dz$ . The pitch and the yaw angles are minimized by counter-directional stage movement, that is, for a displacement vector  $(x, y)$  it yields  $\mathbf{X}_n = \mathbf{X}_{n-1} + (x, -x, y, -y)$ . Figure 4 shows the simulated field profiles along the wire.

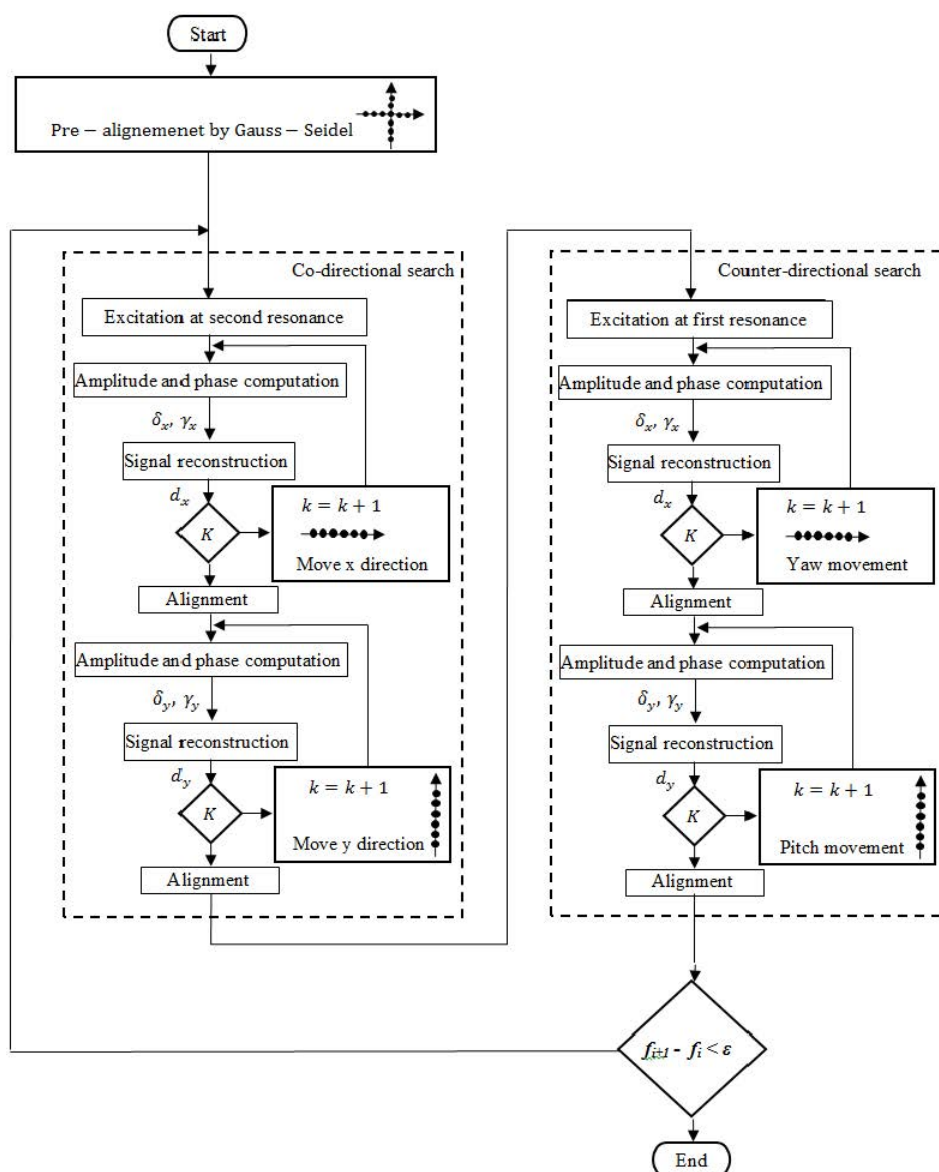
### 2.3 The measurement procedure

Figure 5 shows a diagram of the measurement procedure. A pre-alignment is done by minimizing the wire oscillation at its first and second resonance frequency by means of the Gauss-Seidel line search procedure, also known as coordinate-search [9].

Using the second resonance frequency and co-directional stage movements, the oscillation amplitudes  $\delta_y(k)$  and  $\delta_x(k)$  are acquired step-by-step along  $k = 1, \dots, K$  positions inside the magnet aperture. In order to increase the measurement precision, a linear regression is carried out on the oscillation amplitudes acquired in the  $x$  and  $y$  directions separately. In the optimization process the stage movement is done sequentially for the both coordinate directions until the minimum is found.

Figures 6 show an experimental example of these linear regressions on a solenoid under test, where the wire was 1 mm off axis. Figure 6 (a) shows  $N = 32$  measurements of the the voltage signal from the wire displacement sensors. The voltages were acquired for equally spaced displacements for a total range of 7 mm within the aperture of the magnet. Figure 6 (b) shows the signal according to eq. (2.6). The interception between the linear regression curve and the ordinate yields the distance between the magnetic axis and the zero reference of the wire stages. When the





**Figure 5.** Magnetic axis measurement procedure for solenoid magnets.

wire position coincides with the magnetic axis, a position measurement system is used to refer the axis position to the magnet fiducial markers mechanically attached to the magnet frame.

The procedure continues with measurements acquired by moving the wire stages in counter-directional mode until the pitch and yaw angles are minimized (right hand side in the block-diagram of figure 5). The procedure is then iterated until the change in the objective function drops below a user-supplied threshold.

Figures 7 show a map of the measured oscillation amplitudes  $\delta(x, y) = \sqrt{[\delta_x(x, y)]^2 + [\delta_y(x, y)]^2}$ , using the second resonance and co-directional movement with a grid of 2-by-2 mm and a step resolution of 0.1 mm. Notice the displacement between the reference

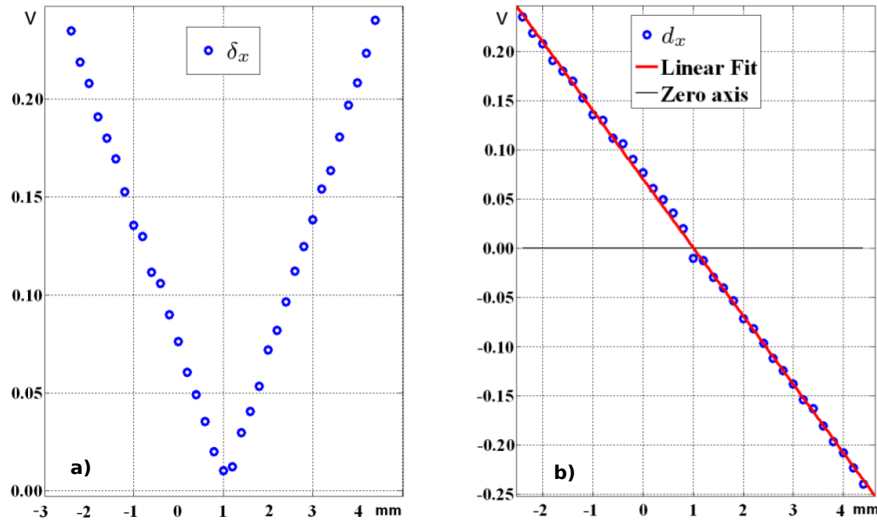


**Figure 6.** Acquired voltages proportional to a)  $\delta_x$ , and b)  $d_x$  (corrected by the phase  $\gamma_x - \frac{\pi}{2}$ ) [10].

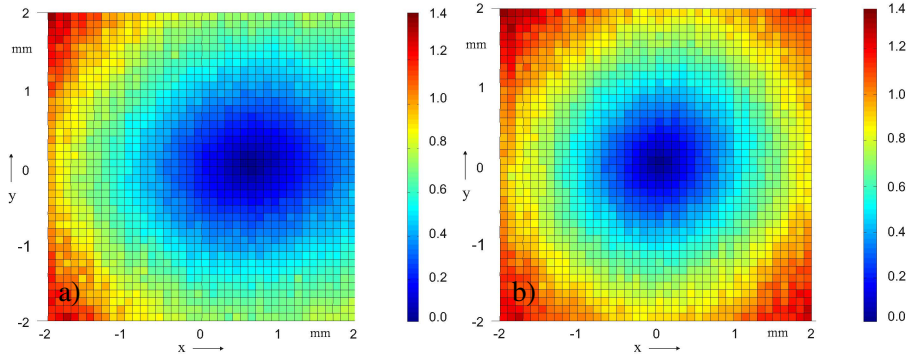


**Figure 7.** Oscillation amplitudes in  $x$  and  $y$ -directions as a function of the wire position with a resolution of 0.1 mm. Wire excitation at second resonance, before (a) and after (b) the magnet centering and alignment.

systems of the stages and the magnet in figure 7 (a). The slight elliptical shape of the map is due to the axis misalignment. Figure 7 (b) shows the situation after centering and alignment.

The components  $\delta_x(x, y)$  and  $\delta_y(x, y)$ , shown separately in figures 8, visualize their linearity with respect to the displacement from the magnet center and motivate the linear regression during each coordinate search.

### 3 Experimental validation of the method

In this section, the results of the experimental validation of the proposed method are illustrated with a solenoid prototype for the Linac4 project at CERN.

#### 3.1 The measurement system

Figure 9 shows the architecture of the measurement system.

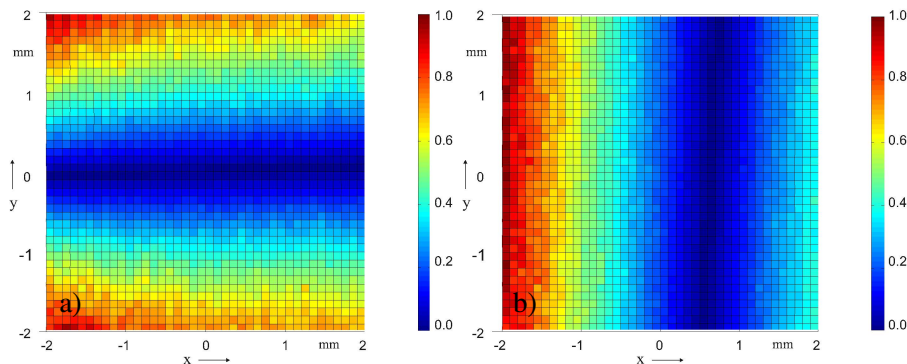


**Figure 8.** Oscillation amplitudes in  $x$  (a) and  $y$ -directions (b), proportional to the integral of the fringe-field along the stretched wire.

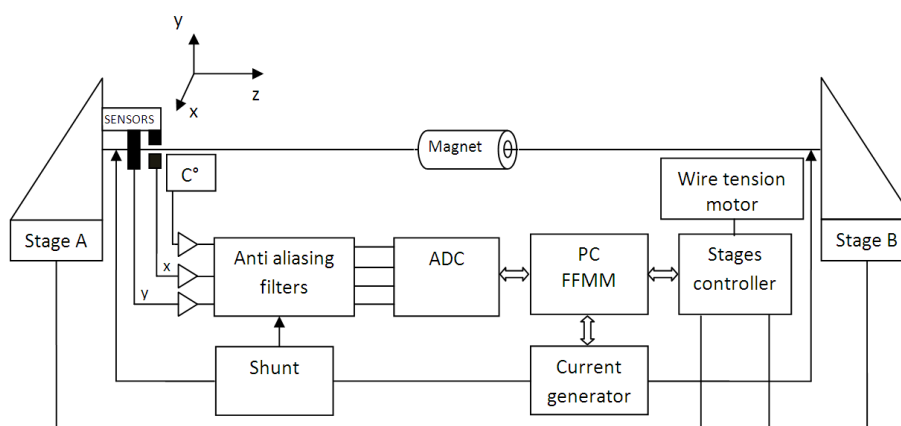


**Figure 9.** Architecture of the oscillating wire system [11].

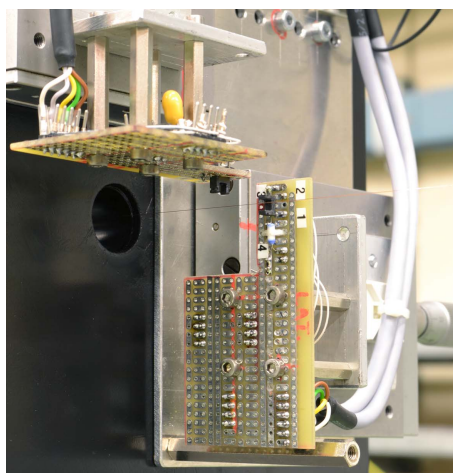
A copper-beryllium (Cu-Be) wire of 0.125 mm in diameter is positioned by two displacement stages (labelled A and B), where the wire end points are fixed by ceramic ball bearings and kept to a floating electrical potential. The main mechanical properties of the wire are given in table 2. The mechanical tension of the wire is controlled by a motor at one end, and by a tension sensor at the other one. The wire can be easily adjusted to the magnet length by moving the stages on a 6-m-long granite bench. The return wire is routed through a field-free region.

A DC motor with a low-friction ball screw eliminates slip-stick effects and delivers displacements with 100-nm incremental motion. Precise position feedback is provided by a linear encoder with 50-nm resolution, mounted in the center of the stage, to eliminate all drive-train induced motion errors.

At each wire position, the peak-to-peak amplitudes of the wire oscillations in directions  $x$  and  $y$  are transduced into a voltage by phototransistors (Sharp<sup>TM</sup> GP1S094HCZ0F), positioned at a right angle close to the fixed point of the wire (at about 100 mm) near the A stage (figure 10). The oscillation amplitude can be derived from the Fourier transform of the sinusoidal voltage signal. In this way, the high-frequency noise from the external environment can be reduced. The mechanical/optical aperture of the photo-transistor determines the maximum oscillation amplitude of about

**Table 2.** Parameters for the mechanical properties of the vibrating wire used in this set up.

Mass density of wire (0.125 mm)	$\rho$	$1.1 \cdot 10^{-4} \text{ kg m}^{-1}$
Damping coefficient	$\alpha$	$1.48 \cdot 10^{-4} \text{ kg m}^{-1} \text{ s}^{-1}$
Wire tension	$T$	9.5 N
Wire length	$L$	1850 mm
Excitation current	$I_0$	105 mA
Second resonance frequency	$f_2$	139.6 Hz

**Figure 10.** Transducers at a right angle to measure the two Cartesian components of the wire motion.

0.3 mm. This, in turn, determines the maximum wire-current amplitude for a given magnetic flux density in the magnet.

The second resonance frequency was measured to be 139.6 Hz by finding the maximum amplitude response as a function of the excitation frequency. The wire was fed by a sinusoidal current with an amplitude current of 105 mA.

The transducer output, pre-amplified and low-pass filtered by an anti-aliasing filter, is sent to the 18-bits acquisition board (National Instruments<sup>TM</sup> NI6289). The same board also acquires the wire-excitation current on a reference resistor. A motor controller is used for acquiring the position through a linear encoder with a precision of  $\pm 0.1 \mu\text{m}$  on a maximum displacement of 150 mm of the stages A and B. The stage controller is driven by the software FFMM [12], the Flexible Framework for Magnetic Measurements, developed at CERN in collaboration with the University of Sannio.

The mechanical positioning of the wire is critical because its uncertainty affects strongly the measurement precision. For this reason, a characterization of the positioning uncertainty was carried out on a circular trajectory. The differences between the setpoints and the reading from the linear encoders are given in figure 11. The precision is of the order of  $\pm 0.1 \mu\text{m}$ , which corresponds to a relative uncertainty of  $\pm 10 \text{ ppm}$ .

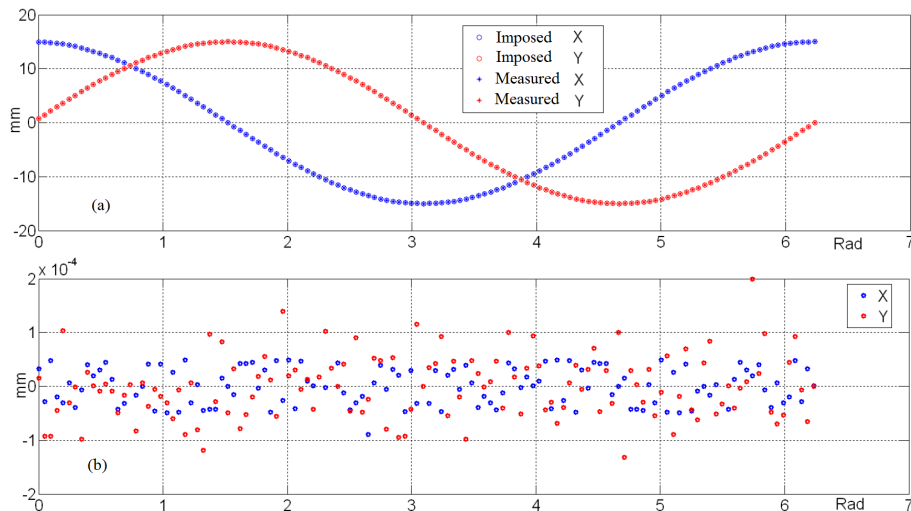


**Figure 11.** (a) Setpoint and measured positions. (b) Differences between setpoints and  $x$  and  $y$  position readout from the linear encoders.

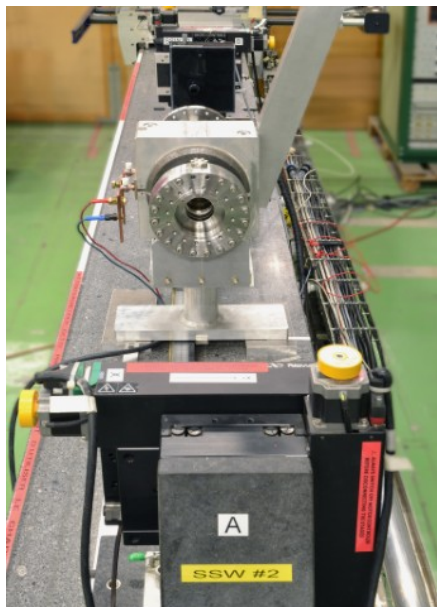


**Figure 12.** Vibrating wire measurement bench with mounted solenoid magnet under test.

### 3.2 Experimental results

Figure 12 shows the granite measurement bench with the mounted solenoid and the two displacement stages for the stretched wire. The tests were carried out for a solenoid excitation current of 20 A in DC. Before the measurements, the magnet was leveled with respect to gravity. Figure 13 shows the sets of measured voltages from the photo-transistors, which correspond to the oscillation amplitudes, for co-directional stage movements with steps of 0.1 mm. This value is compatible with the uncertainty of the fiducial marker position, measured by means of an optical laser system. The initial misalignment of the magnet center in the horizontal plane, causing vertical wire oscil-

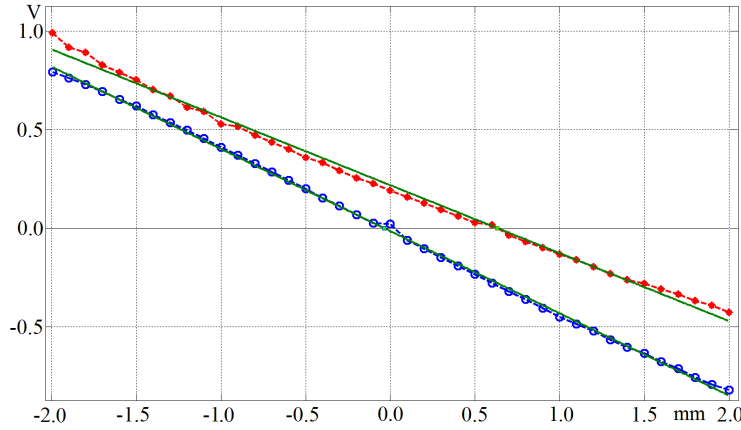


**Figure 13.** Photo-transistor voltage (proportional to the wire oscillation amplitude) as a function of the stage position during the co-directional line search. Horizontal (o) and vertical measurements (\*), together with the linear regression curves.

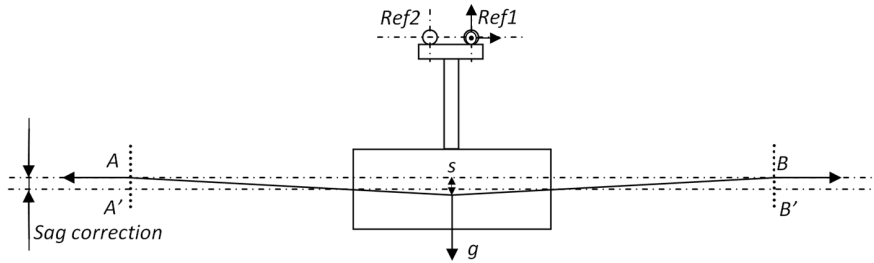


**Figure 14.** Correcting the vertical axis position measurement for the wire sag.

lations, was found to be of the order of 0.6 mm. The initial vertical misalignment was found to be one order of magnitude smaller.

Experience has shown that three iterations between the co- and counter directional movements are sufficient to center and align the magnet with a precision higher than it is achievable with a laser tracker system for the mechanical referencing of the magnet structure with respect to the measurement stages. Knowing the wire length and the natural resonance frequency, the sag of the wire,  $s$ , can be calculated by [13]:

$$s = \frac{g}{32f^2}, \quad (3.1)$$

where  $g$  is the gravity constant ( $9.807 \text{ m s}^{-2}$ ) and  $f$  is the natural wire resonance frequency. In this case,  $f$  is equal to 69.7 Hz and therefore the sag is 0.063 mm, which cannot be neglected. Figure 14 shows the scheme for correcting the vertical axis position of the stages when a non-negligible sag is present. Henceforth, the offset of the fiducial reference markers (denoted as  $\text{Ref}_1$  and  $\text{Ref}_2$ ), where the local coordinate system of the magnet is fixed, is given as a function of the stage positions  $A'$  and  $B'$ .

The mounting scheme of the magnet on the measurement bench and the location of the fiducial reference markers are shown schematically in figure 15. The alignment with respect to the  $x$  axis is carried out by means of a gravity sensor, which will be done also on the alignment girder in the

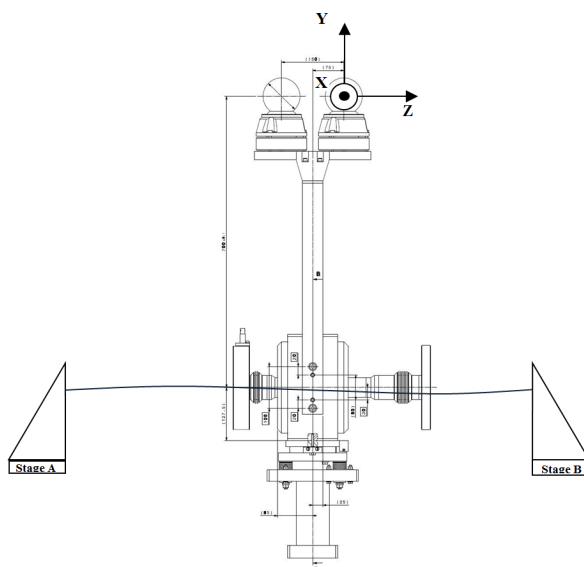


**Figure 15.** Mounting scheme of the magnet on the measurement bench and location of the fiducial reference markers.

**Table 3.** Optical measurement with respect to the reference point on the magnet.

	X (mm)	Y (mm)	Z (mm)
Ref <sub>1</sub>	0.00	0.00	0.00
Ref <sub>2</sub>	0.00	0.00	-149.98
A'	-206.87	-628.07	994.69
B'	-206.87	-628.07	994.69

accelerator. In this way, the two markers are sufficient for the alignment with respect to pitch and yaw angles, that is, rotations about the axes  $x$  (horizontal plane) and  $y$  (vertical plane). The values of the position measurement achieved by the optical Leica system are given in table 3.

The misalignment between the magnetic axis and the geometrical axis, measured with respect to the fiducial markers, is  $-5.26$  mrad in the horizontal plane (yaw) and  $2.18$  mrad in the vertical plane (pitch).

#### 4 Conclusions

A method to center and align a solenoid by means of a vibrating wire is proposed. A copper beryllium wire, fed by an alternating current, oscillates in a plane perpendicular to the transverse magnetic field inside the aperture of the solenoid. The amplitude of this oscillation is proportional to the current and field magnitudes. When the magnetic axis coincides with the wire position, the transverse magnetic field components along the wire cancel out and therefore no motion is induced. A sinusoidal current of the second wire-resonance frequency yields sensitivity in the micrometer range.

Care must be taken that the wire tension, which is related to the resonance frequency, remains constant during the co- and counter-directional movements of the stages. The maximum possible displacement of the stages is furthermore affected by the alignment between the wire and the photo-transistors.

The method has been validated by centering and aligning a solenoid for the project Linac4 at CERN. The measured oscillation amplitudes are sensitive to displacements at the wire stages of the order of  $0.1 \mu\text{m}$ . Once the magnetic axis is found, it must be related to the geometric axis defined by the position of two fiducial reference markers attached to the magnet yoke. This can be done by means of a laser tracker system with an accuracy of about  $10 \mu\text{m}$  or with sensing heads of  $1 \mu\text{m}$ .

## Acknowledgments

The authors would like to thank P. Galbraith for his experimental contribution to set up the equipment.

## References

- [1] A.N. Mirzoian, P.N. Ostroumov, G.V. Romanov and A.P. Fateev, *Increase of injection efficiency in a high current linear proton accelerator*, *J. Tech. Phys.* **25** (1980) 710.
- [2] J. Buckley, D. Richter, L. Walckiers and R. Wolf, *Dynamic Magnetic Measurements of Superconducting Magnets for the LHC*, *IEEE T. Appl. Supercon* **5** (1995) 1024.
- [3] J. DiMarco, *MTF Single Stretched Wire System*, MTF-96-0001 (1996).
- [4] A. Jain et al., *A Vibrating Wire R&D For Alignment of Multipole Magnets in NSLS-II*, in proceedings of 10<sup>th</sup> International Workshop on Accelerator Alignment, KEK, Tsukuba, Japan (2008).
- [5] A. Temnykh, Y. Levashovb and Z. Wolf, *A Study of undulator magnets characterization using the Vibrating Wire technique*, *LCLS-TN-10-2* (2010).
- [6] J. DiMarco et al., *Solenoid Measurements with SSW*, in proceedings of 15<sup>th</sup> International Magnetic Measurement Workshop (IMMW) (2007).
- [7] J. DiMarco et al., *Solenoid Magnet Alignment at Fermilab*, in proceedings of 16<sup>th</sup> International Magnetic Measurement Workshop (IMMW) (2009).
- [8] J. DiMarco, H. Glass, M.J. Lamm, P. Schlabach, C. Sylvester, J.C. Tompkins and J. Krzywinski, *Field alignment of quadrupole magnets for the LHC interaction regions*, *IEEE T. Appl. Supercon.* **10** (2000) 127.
- [9] S. Russenschuck, *Field Computation for Accelerator Magnets. Analytical and Numerical Methods for Electromagnetic Design and Optimization*, WILEY-VCH Verlag GmbH, Weinheim, Germany (2010).
- [10] P. Arpaia, C. Petrone and L. Walckiers, *Experimental validation of solenoid magnetic centre measurement by vibrating wire system*, in proceedings of XX IMEKO World Congress Metrology for Green Growth, Busan, Republic of Korea (2012).
- [11] P. Arpaia, M. Buzio, J. Garcia Perez, C. Petrone, S. Russenschuck and L. Walckiers, *Measuring field multipoles in accelerator magnets with small-apertures by an oscillating wire moved on a circular trajectory*, *2012 JINST* **7** P05003.
- [12] P. Arpaia, M. Buzio, L. Fiscarelli and V. Inglese, *A software framework for developing measurement applications under variable requirements*, *Rev. Sci. Instrum.* **83** (2012) 115103.
- [13] Z. Wolf, *A Vibrating Wire System For Quadrupole Fiducialization*, *LCLS-TN-05-1* (2005).